

Vibration control of the coal pulverizer geared drive system using linear actuators with the magneto-rheological fluid

Tomasz Szolc¹, Łukasz Jankowski², Andrzej Pochanke³, Maciej Michajłow⁴

^{1,2,4} Institute of Fundamental Technological Research of the Polish Academy of Sciences, ul. Pawińskiego 5 B, 02-106 Warsaw, Poland, ¹tszolc@ippt.gov.pl, ²ljank@ippt.gov.pl, ⁴m.michajlow@gmail.com

³ Department Faculty of Electrical Engineering of the Warsaw University of Technology, Plac Politechniki 1, 00-661 Warsaw, Poland, e-mail: andrzej.pochanke@ee.pw.edu.pl

Abstract

Torsional vibrations are in general rather troublesome to control from the viewpoint of proper control torque generation as well as because of difficulties of imposing the control torques on quickly rotating parts of the drive- or rotor-shaft systems. In this paper there is proposed an active control technique based on the linear actuators with the magneto-rheological fluid (MRF) connecting the drive system planetary gear housing with the immovable rigid support. Here, by means of the magneto-rheological fluid of adjustable viscosity control damping torques are generated. Such actuators can effectively suppress amplitudes of severe transient and steady-state rotational fluctuations of the gear housing position and in this way they are able to minimize dangerous oscillations of dynamic torques transmitted by successive shaft segments in the entire drive system. The general purpose of the considerations is to control torsional vibrations of the power-station coal-pulverizer drive system driven by means of the asynchronous motor and the single stage planetary gear. In the computational examples drive system transient torsional vibrations induced by the electromagnetic motor torques during start-ups as well as steady-state vibrations excited by the variable dynamic retarding torques generated by the coal pulverizer during nominal operation have been significantly attenuated.

1 Introduction

From among various kinds of vibrations occurring in drive systems of machines, mechanisms and vehicles the torsional ones are very important as naturally associated with their fundamental rotational motion. Torsional vibrations of drive trains are very dangerous for material fatigue of the most heavily affected and responsible elements of these mechanical systems. Thus, this problem has been considered for many years by many authors, not only in numerous research papers, but also in the monographic form, e.g. in [1]. Active vibration control of drive systems of rotating machines, mechanisms and vehicles creates new possibilities of improvement of their effective operation. Torsional vibrations are in general rather difficult to control not only from the viewpoint of proper control torque generation, but also from the point of view of a convenient technique of imposing the control torques on quickly rotating parts of the drive-systems and rotor machines. Unfortunately, one can find not so many published results of research in this field, beyond some attempts performed by active control of shaft torsional vibrations using piezo-electric actuators, [2]. But in such cases relatively small values of control torques can be generated and thus the piezo-electric actuators can be usually applied to low-power drive systems. Moreover, even if a relatively large number of the piezo-electric actuators are attached to the rotor-shafts of the entire drive system, as it follows e.g. from [2], only higher eigenmodes can be controlled, whereas control of the most important fundamental eigenmodes is often not sufficiently effective. At present, the rotary actuators in the form of torsional dampers usually are not able to generate sufficiently great retarding torque values required to control the high-power drive systems. In [3,4] there was proposed the semi-active control technique based on the actuators in the form of rotary dampers with the magneto-rheological fluid (MRF). In these actuators between the shaft and the inertial ring, which is freely rotating with a velocity close or equal to the system average rotational speed, the magneto-rheological fluid of adjustable viscosity is used. Such actuators generate control torques that are functions of the shaft actual rotational speed, which consist of the average component corresponding to the rigid body motion and of the fluctuating component caused by the torsional vibrations. In

an engineering practice, by means of this approach one can effectively attenuate torsional vibrations in rotating systems transmitting power values not exceeding $5 \div 10$ kW, which follows from [4].

Thus, for drive systems of high-power machines, mechanisms and vehicles in this paper there is proposed the active control technique based on the linear actuators with the magneto-rheological fluid (MRF) connecting the drive system planetary gear housing with the immovable rigid support. The control torques are generated by means of the magneto-rheological fluid of adjustable viscosity. They interact with reaction torques transmitted by the planetary gear housing due to torsional vibrations of the drive system. Such actuators can effectively suppress amplitudes of severe transient and steady-state rotational fluctuations of the gear housing position and in this way they are able to minimize dangerous oscillations of dynamic torques transmitted by successive shaft segments in the entire drive system.



Figure 1: Coal pulverizer drive system (a) and the damper with the linear MRF actuators (b)

The general purpose of the considerations is to control torsional vibrations of the power-station coal-pulverizer drive system driven by means of the asynchronous motor and the double stage planetary gear shown in Fig. 1a. The planetary gear housing is visco-elastically connected with the immovable foundation by means of two or four linear actuators with the magneto-rheological fluid, as illustrated in Figs. 1a and 1b. The actuators support the gear housing at both ends of the proper reaction arm enabling it bounded rotational displacements around the drive system rotation axis. Using such suspension of the gear housing control forces generated by the linear actuators can be applied to the drive system in the form of control torques.

In order to develop sufficiently reliable control algorithms for the considered drive system, the theoretical investigations are performed by means of its two structural mechanical models: the hybrid one and the classical finite element (FEM) model as well as using sensitivity analysis of the responses with respect to the linear actuator control characteristics. The electrical vibrations are investigated here in order to determine in a possibly accurate way the electromagnetic driving torque produced by the asynchronous motor, which is particularly essential for reliable active vibration control. For this purpose there is applied the proper electrical model of the asynchronous motor in the form of Park's circuit-type ordinary differential equations coupled with the motion equations of both abovementioned mechanical models of the coal pulverizer drive system. Thus, these models can be called the electro-mechanical models. In the computational examples there are going to be effectively suppressed the transient torsional vibrations of the drive system induced by the electromagnetic motor torques during start-ups as well as the steady-state vibrations excited by the variable dynamic retarding torques generated by the coal pulverizer working tool during nominal operation.

2 Assumptions for the mechanical models and formulation of the problem

In the considered drive system of the coal pulverizer power is transmitted from the asynchronous motor to the driven machine tool by means of the three elastic couplings, double-stage planetary reduction gear, two torque-meters, electro-magnetic overload coupling and by the shaft segments. As mentioned above, the planetary gear housing is visco-elastically connected with the foundation by means of two or four linear magneto-rheological actuators of controllable damping properties and adjustable stiffness, which enable us to properly tune-up the drive train to the natural frequency values. The considered real drive system is presented in Fig. 1a. Its corresponding mechanical model is shown in Fig. 2.

In order to perform a theoretical investigation of the semi-active control applied for this mechanical system, a reliable and computationally efficient simulation models are required. In this paper dynamic investigations of the entire drive system are performed by means of two structural models consisting of torsionally deformable one-dimensional beam-type finite elements and rigid bodies. These are the discrete-continuous (hybrid) model

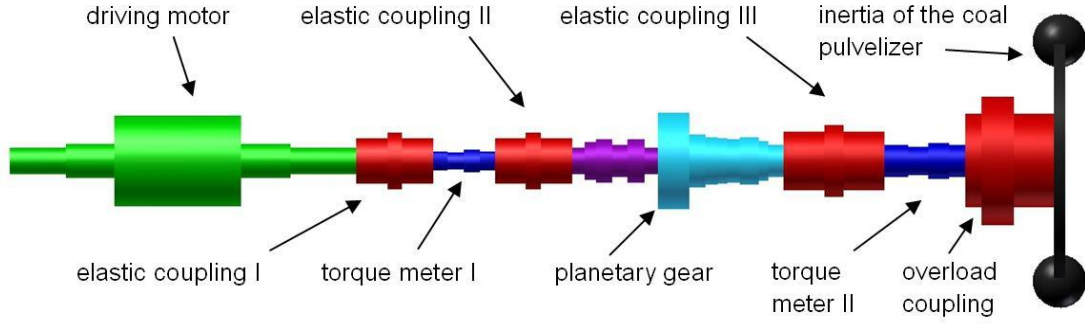


Figure2: Mechanical model of the coal pulverizer drive system

and the classical finite element model. Both models are characterized by the identical structure resulting in the same division into cylindrical beam elements representing successive drive train components, which can be illustrated in common Fig. 2. These models are employed here for eigenvalue analyses as well as for numerical simulations of torsional vibrations of the drive train. In the hybrid model successive cylindrical segments of the stepped rotor-shaft are substituted by the cylindrical macro-elements of continuously distributed inertial-visco-elastic properties, as presented in Fig. 2. However, in the finite element model these continuous macro-elements have been discretized with a proper mesh density assuring a sufficient accuracy of results. Since in the real drive system the electric motor coils and coupling disks are attached along some rotor-shaft segments by means of shrink-fit connections, the entire inertia of such components is increased, whereas usually the shaft cross-sections only are affected by elastic deformations due to transmitted loadings. Thus, the corresponding visco-elastic macro-elements in the hybrid model and the discretized finite elements in the FEM model must be characterized by the geometric cross-sectional polar moments of inertia J_{Ei} responsible for their elastic and inertial properties as well as by the separate layers of the polar moments of inertia J_{Ii} responsible for their inertial properties only, $i=1,2,\dots,n$, where n is the total number of macro-elements in the considered hybrid model. In the proposed hybrid and FEM model of the coal pulverizer drive system inertias of the gear wheels, gear housing with the reaction arm, coupling disks and others are represented by rigid bodies attached to the appropriate macro-element extreme cross-sections, which should assure a reasonable accuracy for practical purposes. The time- and response-dependent external active and passive torques are continuously distributed along the respective macro-elements or imposed in the concentrated form to the given macro-element cross-sections.

Similarly as in [3,4], angular displacements $\theta_i(x,t)$ with respect to the shaft rotation with the average angular velocity Ω of cross-sections of each visco-elastic macro-element in the hybrid model are governed by the hyperbolic partial differential equations of the wave type, where x is the spatial co-ordinate and t denotes time. Mutual connections of the successive macro-elements creating the stepped shaft as well as their interactions with the rigid bodies are described by equations of boundary conditions. These equations contain geometrical conditions of conformity for rotational displacements of the extreme cross sections for $x=L_i=l_1+l_2+\dots+l_{i-1}$ of the adjacent $(i-1)$ -th and the i -th elastic macro-elements:

$$\theta_{i-1}(x,t) = \theta_i(x,t) \quad \text{for } x = L_i. \quad (1a)$$

The second group of boundary conditions are dynamic ones, which contain equations of equilibrium for external and control torques as well as for inertial, elastic and external damping moments. For example, the dynamic boundary condition describing a simple connection of the mentioned adjacent $(i-1)$ -th and the i -th elastic macro-elements has the following form:

$$I_{0i} \frac{\partial^2 \theta_i}{\partial t^2} - G_i J_{Ei} \left(1 + \tau \frac{\partial}{\partial t} \right) \frac{\partial \theta_i}{\partial x} + G_{i-1} J_{E,i-1} \left(1 + \tau \frac{\partial}{\partial t} \right) \frac{\partial \theta_{i-1}}{\partial x} = 0 \quad (1b)$$

for $x = L_i, \quad i = 2,3,\dots,n,$

where I_{0i} is the mass polar moment of inertia of the rigid body, if any, attached in the considered cross-section, τ denotes the retardation time in the Voigt model of material damping, G_i denotes the Kirchhhoff's modulus of the rotor-shaft material.

The elastically supported planetary gear in the drive system hybrid model has been also described by the boundary conditions. This gear model is schematically illustrated in Fig. 3. Since in the performed considerations the lower range of vibration frequencies is going to be investigated, in the proposed models the gear mesh flexibilities responsible for rather higher frequency dynamic effects have been neglected. Thus, for the planetary gear stage located between the $k-1$ -th and the k -th beam macro-element the proper geometric boundary

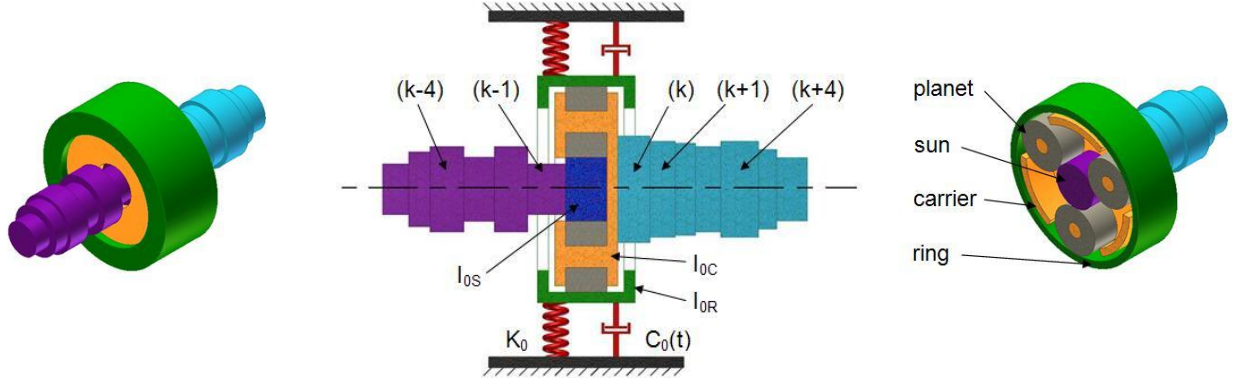


Figure 3: Modeling of the elastically supported planetary gear

condition follows from the Willis' formula, [1]

$$\theta_{k-1}(x, t) = \kappa \theta_k(x, t) - r_{RS} \varphi_R(t), \quad \kappa = 1 + \frac{r_R}{r_S}, \quad r_{RS} = \frac{r_R}{r_S} \quad \text{for } x = L_k, \quad (2a)$$

where $\theta_{k-1}(L_k, t)$ corresponds to the rotational displacement of the sun gear, $\theta_k(L_k, t)$ corresponds to the rotational displacement of the carrier, $\varphi_R(t)$ denotes the angular displacement of the elastically supported gear housing and r_R , r_S are the radii of the ring and sun gear wheels, respectively. Dynamic behavior of such a planetary gear is described by the following equations of equilibrium

$$\left(I_{0C} + \kappa^2 I_{0S} \right) \frac{\partial^2 \theta_k}{\partial t^2} - \kappa r_{RS} I_{0S} \frac{d^2 \varphi_R}{dt^2} - G_k J_{Ek} \left(1 + \tau \frac{\partial}{\partial t} \right) \frac{\partial \theta_k}{\partial x} + \kappa G_{k-1} J_{E,k-1} \left(1 + \tau \frac{\partial}{\partial t} \right) \frac{\partial \theta_{k-1}}{\partial x} = 0, \quad (2b)$$

$$\left(I_{0R} + r_{RS}^2 I_{0S} \right) \frac{d^2 \varphi_R}{dt^2} - \kappa r_{RS} I_{0S} \frac{\partial^2 \theta_k}{\partial t^2} + C_0(t) \frac{d \varphi_R}{dt} + K_0 \varphi_R - r_{RS} G_{k-1} J_{E,k-1} \left(1 + \tau \frac{\partial}{\partial t} \right) \frac{\partial \theta_{k-1}}{\partial x} = 0 \quad \text{for } x = L_k, \quad (2c)$$

where I_{0S} , I_{0C} and I_{0R} denote respectively the mass moments of inertia of the rigid bodies representing the sun gear, carrier and the gear housing together with the ring wheel and the reaction arm, K_0 is the adjustable gear housing support rotational stiffness and $C_0(t)$ denotes the variable control viscosity coefficient dependent on the current properties of the magneto-rheological fluid in the linear actuators. Analogous relationships describing the planetary gear in the finite element model can be derived by means of the Lagrange equations.

In order to perform an analysis of natural elastic vibrations, all the forcing and viscous terms in the motion equations and boundary condition (2c) have been omitted. An application of the analytical solution of variable separation leads to the following characteristic equation for the considered eigenvalue problem:

$$\mathbf{C}(\omega) \cdot \mathbf{D} = \mathbf{0}, \quad (3)$$

where $\mathbf{C}(\omega)$ is the real characteristic matrix and \mathbf{D} denotes the vector of unknown constant coefficients in the analytical local eigenfunctions of each i -th macro-element. Thus, the determination of natural frequencies reduces to the search for values of ω , for which the characteristic determinant of matrix \mathbf{C} is equal to zero. Then, the torsional eigenmode functions are obtained by solving equation (3).

Similarly as in [3,4], the solution for forced vibration analysis has been obtained using the analytical - computational approach. Solving the differential eigenvalue problem (1)-(3) and an application of the Fourier solution in the form of series in the orthogonal eigenfunctions lead to the set of uncoupled modal equations for time coordinates $\xi_m(t)$. The damping torque $-C_0(t)\varphi'_R(t)$ standing in Equation (2c) can be regarded as the response-dependent control external excitation. Then, by a transformation of it into the space of modal coordinates $\xi_m(t)$ and upon a proper rearrangement of the modal independent equations, the following set of coupled modal equations is yielded:

$$\mathbf{M}_0 \ddot{\mathbf{r}}(t) + \mathbf{D}(C_0(t)) \dot{\mathbf{r}}(t) + \mathbf{K}_0 \mathbf{r}(t) = \mathbf{F}(t, \dot{\mathbf{r}}(t)), \quad (4)$$

where $\mathbf{D}(C_0(t)) = \mathbf{D}_0 + \mathbf{D}_C(C_0(t)\dot{\mathbf{r}}(t))$.

The symbols \mathbf{M}_0 , \mathbf{K}_0 and \mathbf{D}_0 denote, respectively, the constant diagonal modal mass, stiffness and damping matrices. The full matrix $\mathbf{D}_C(C_0(t))$ plays here a role of the semi-active control matrix and the symbol $\mathbf{F}(t, \dot{\mathbf{r}}(t))$ denotes the response dependent external excitation vector due to the electromagnetic torque generated by the

electric motor and due to the retarding torque produced by the driven coal pulverizer. The Lagrange coordinate vector $\mathbf{r}(t)$ consists of the unknown time functions $\xi_m(t)$ in the Fourier solutions, $m=1,2,\dots$. The number of equations (4) corresponds to the number of the torsional eigenmodes taken into consideration in the range of frequency of interest. These equations are mutually coupled by the out-of-diagonal terms in matrix \mathbf{D} regarded as external excitations expanded in series in the base of orthogonal analytical eigenfunctions. A fast convergence of the applied Fourier solution enables us to reduce the appropriate number of the modal equations to solve in order to obtain a sufficient accuracy of results in the given range of frequency. Here, it is necessary to solve only 6÷10 coupled modal equations (4), contrary to the classical one-dimensional rod finite element formulation leading in general to a relatively large number of motion equations in the generalized coordinates.

For the assumed analogous linear finite element model the mathematical description of its motion has the classical form of a set of coupled ordinary differential equations

$$\mathbf{M}\ddot{\mathbf{s}}(t) + \mathbf{C}\left(C_0(t)\dot{\mathbf{s}}(t)\right)\dot{\mathbf{s}}(t) + \mathbf{K}\mathbf{s}(t) = \mathbf{F}(t, \mathbf{s}(t), \dot{\mathbf{s}}(t)), \quad (5)$$

where $\mathbf{s}(t)$ denotes the vector of generalized co-ordinates $s_j(t)$, \mathbf{M} , \mathbf{C} and \mathbf{K} are respectively the mass, damping and stiffness matrices and \mathbf{F} denotes the time – and system response – dependent external excitation vector. By means of Eqs. (5) numerical simulations of the forced torsional vibrations for the passive and controlled system can be carried out. In order to determine natural frequencies and eigenvectors for the FEM model of this drive system it is necessary to reduce (5) into the form of standard eigenvalue problem. It is to notice here, that the dynamic responses and their control are going to be investigated in the space of modal functions in the case of the hybrid model and in the domain of generalized co-ordinates in the case of the FEM model application.

3. Modeling of the electrical external excitation generated by the asynchronous motor

The torsional vibrations of the drive system usually result in significant fluctuation of rotational speed of the rotor of the driving electric motor. Such oscillation of the angular velocity superimposed on the average rotor rotational speed cause more or less severe perturbation of the electro-magnetic flux and thus additional oscillation of the electric currents in the motor windings. Then, the generated electromagnetic torque is also characterized by additional variable in time components which induce torsional vibrations of the drive system. According to the above, the mechanical vibrations of the drive system become coupled with the electrical vibrations of the currents in the motor windings. Thus, in order to develop a proper control algorithm for the given vibrating drive system the electromagnetic external excitation produced by the motor should be described possibly accurately and thus the electromechanical coupling between the electric motor and the torsional train ought to be taken into consideration. According to the above, apart of the sufficiently realistic mechanical models of the vibrating object, it is also necessary to introduce a proper mathematical model of the electric motor. In the considered case of the symmetrical three-phase asynchronous motor electric current oscillations in its windings are described by six voltage equations, which can be found e.g. in [5]. They can be transformed into the system of four Park's equations

$$\begin{bmatrix} \sqrt{\frac{3}{2}}U \cos(2\pi f_0 t) \\ \sqrt{\frac{3}{2}}U \sin(2\pi f_0 t) \\ 0 \\ 0 \end{bmatrix} = \begin{bmatrix} L_1 + \frac{1}{2}M & 0 & \frac{3}{2}M \cos(p\vartheta) & -\frac{3}{2}M \sin(p\vartheta) \\ 0 & L_1 + \frac{1}{2}M & \frac{3}{2}M \sin(p\vartheta) & \frac{3}{2}M \cos(p\vartheta) \\ \frac{3}{2}M \cos(p\vartheta) & \frac{3}{2}M \sin(p\vartheta) & L_2' + \frac{1}{2}M & 0 \\ -\frac{3}{2}M \sin(p\vartheta) & \frac{3}{2}M \cos(p\vartheta) & 0 & L_2' + \frac{1}{2}M \end{bmatrix} \cdot \begin{bmatrix} i_\alpha^s(t) \\ i_\beta^s(t) \\ i_\alpha^r(t) \\ i_\beta^r(t) \end{bmatrix} + \begin{bmatrix} R_1 & 0 & -\frac{3}{2}pM\Omega(t)\sin(p\vartheta) & -\frac{3}{2}pM\Omega(t)\cos(p\vartheta) \\ 0 & R_1 & \frac{3}{2}M\Omega(t)\cos(p\vartheta) & -\frac{3}{2}M\Omega(t)\sin(p\vartheta) \\ -\frac{3}{2}pM\Omega(t)\sin(p\vartheta) & \frac{3}{2}pM\Omega(t)\cos(p\vartheta) & R_2' & 0 \\ -\frac{3}{2}pM\Omega(t)\cos(p\vartheta) & -\frac{3}{2}pM\Omega(t)\sin(p\vartheta) & 0 & R_2' \end{bmatrix} \cdot \begin{bmatrix} i_\alpha^s(t) \\ i_\beta^s(t) \\ i_\alpha^r(t) \\ i_\beta^r(t) \end{bmatrix}, \quad (6)$$

where U denotes the power supply voltage, f_0 is the electric network frequency, L_1 , L_2' are the stator coil inductance and the equivalent rotor coil inductance, respectively, M denotes the relative rotor-to-stator coil inductance, R_1 , R_2' are the stator coil resistance and the equivalent rotor coil resistance, respectively, p is the number of pairs of the motor magnetic poles, $\vartheta=\vartheta(t)$ denotes the rotation angle between the rotor and the stator, $\Omega(t)$ is the current rotor angular velocity including the average and vibratory component and i_γ^q , $\gamma=\alpha,\beta$, are the electric currents in the rotor for $q=r$ and the stator for $q=s$ reduced to the electric field equivalent axes α and β , [5]. Then, the electromagnetic torque generated by such a motor can be expressed by the following formula:

$$T_{el} = \frac{3}{2} p M \left[(i_{\beta}^s i_{\alpha}^r - i_{\alpha}^s i_{\beta}^r) \cos p\vartheta - (i_{\alpha}^s i_{\alpha}^r + i_{\beta}^s i_{\beta}^r) \sin p\vartheta \right]. \quad (7)$$

From the system of voltage equations (6) as well as from formula (7) it follows that the coupling between the electric and the mechanical system is non-linear in character, which leads to complicated analytical description resulting in a rather complicated computer implementation. Thus, this electromechanical coupling has been realized here by means of the step-by-step numerical extrapolation technique, which for relatively small direct integration steps for equations (4) and (5) results in very effective, stable and reliable results of computer simulation.

4. Computational example

In the computational examples there are investigated start-ups and following after them steady-state operation of the considered drive system of the real coal pulverizer. This system presented in Fig. 1a is accelerated from a standstill to the nominal operating conditions characterized by the rated retarding torque $M_n=143$ Nm at the constant rotational speed 1465 rpm of the motor shaft. The reduction planetary gear ratio is equal to 4.25. In order to imitate the operation of the coal pulverizer in a possibly realistic way, the retarding torque produced by the machine working tool has been assumed as linearly proportional to the current shaft rotational speed with a superimposed step-wise fluctuation component of also velocity-dependent amplitude

$$M_r(\Omega_r(t)) = \frac{M_n}{\Omega_n} \Omega_r(t) \cdot \left(1 + z \cdot \text{sgn}(\sin(k\vartheta_r(t))) \right), \quad (8)$$

where Ω_n denotes the nominal angular velocity, $\Omega_r(t)$ is the current angular velocity of the working tool, h denotes the step fluctuation ratio, $\vartheta_r(t)$ is the working tool current phase angle and z denotes the frequency parameter of the retarding torque oscillation. It is to remark that function (8) describing the assumed retarding torque consists of the average component expressing a mean resistance of the comminuted coal of a given average density and of the fluctuating one, which represents rapid changes of the braking moment caused by a non-homogeneous structure of the pulverized material. Here, for temporary negative values of the retarding torque $M_r(t)$ is assumed to be equal to zero. The electromagnetic torque (7) generated by the asynchronous motor is assumed to be uniformly distributed along the mechanical model elements corresponding to the motor rotor. However, the retarding torque (8) is imposed in a concentrated form to the rigid body representing inertia of the coal pulverizer working tool, Fig. 2.

The qualitative dynamic properties of the considered drive system have been determined first in the form of an eigenvalue analysis by solving equation (3). In Fig. 4 there are depicted the lowest for this system first four eigenfunctions together with the corresponding natural frequency values obtained for the classical rigid support of the gear housing with the foundation. All these eigenforms are contained in the frequency range 0÷200 Hz which is fundamental from the viewpoint of an effective control of the most severe torsional vibrations. In this figure the modal displacement of the rigid body representing the gear housing is depicted by means of the vertical bar located at the gear stage position corresponding to the length abscissa 1.25 m. It is to notice that for

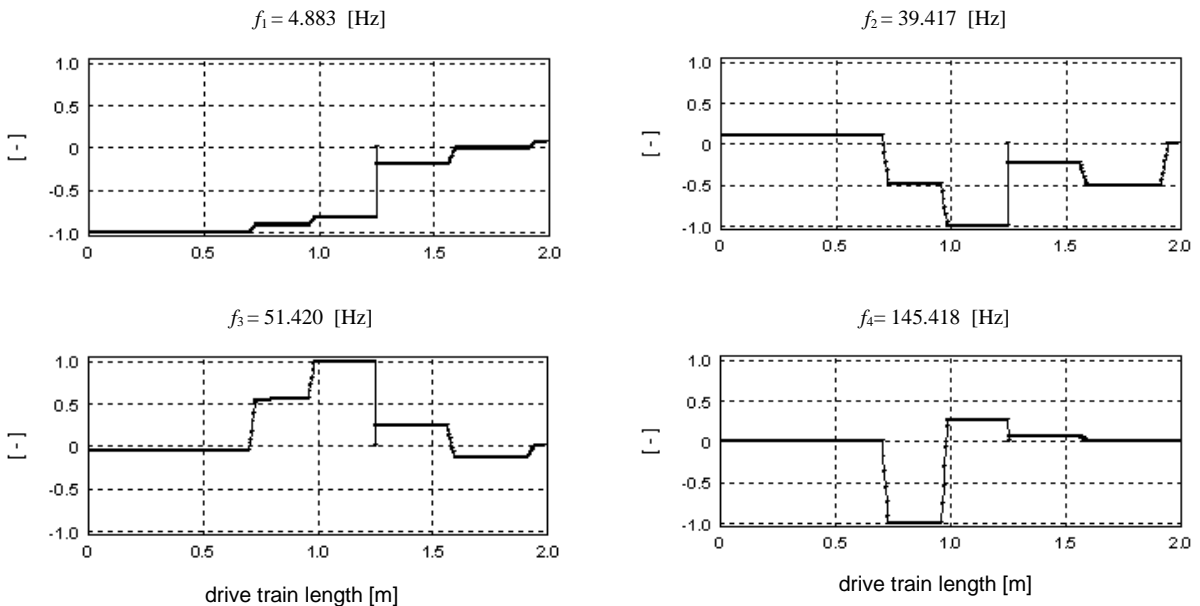


Figure 4: Eigenfuctions with the corresponding natural frequencies of the drive system with a rigid support of the gear housing

the assumed gear housing rigid support this modal angular displacement is equal to zero in all four cases of eigenfunctions, Fig. 4. From shapes of these eigenfunctions it follows that beyond the first one of frequency $f_1 = 4.883$ Hz all remaining ones are hardly excited by the driving motor and by the retarding torques generated by the coal pulverizer working tool as well as an influence of the mentioned three elastic couplings in the drive train on its eigenforms is very significant. The next eigenfunctions are characterized by much higher natural frequencies exceeding 760 Hz and they seem to be of secondary importance from the viewpoint of the investigated here dynamic processes.

In Fig. 5 in there are presented analogous eigenfunctions of the considered drive system with elastically supported gear housing by means of the two magneto-rheological dampers, which have the rotational suspension stiffness of $K_0 = 0.79 \cdot 10^4$ Nm/rad. In the mentioned frequency range 0÷200 Hz the number of these eigenforms has increased to five. Here, the elastic support of the gear housing results in a slight decrease of the natural frequency values corresponding to the first three eigenforms. The fourth eigenform of frequency $f_4 = 92.248$ Hz is the “new” one introduced by the applied elastic rotational foundation of the gear housing characterized by its relatively high modal displacement equal ca. 0.75, Fig. 5. All these eigenfunctions have non-zero values of the gear housing modal displacement, which enables us to introduce additional controllable absolute housing-to-foundation damping into the coal pulverizer drive system. It is to emphasize that all eigenfunctions presented in Figs. 4 and 5 respectively almost overlay with the corresponding plots of eigenvectors obtained using the FEM model of this drive system consisting of 215 two-node rod elements, where the respective differences of successive natural frequencies did not exceed 0.1 %.

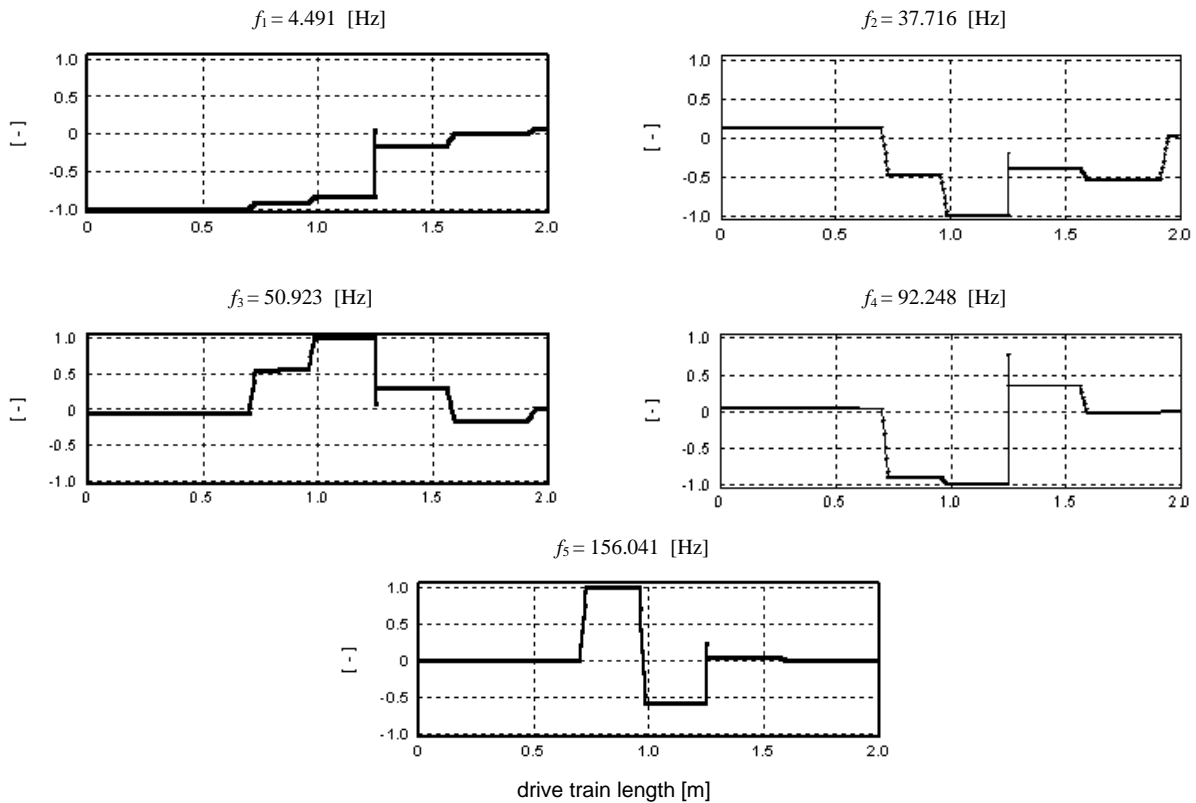


Figure 5: Eigenfuctions with the corresponding natural frequencies of the drive system with an elastic support of the gear housing

The transient and steady-state torsional vibrations of the coal pulverizer drive system are excited here by the electromagnetic torque generated by the asynchronous motor and determined using formula (7) during numerical simulations of the start-up and nominal operation process regarding the torsional vibrations of the mechanical system as mutually coupled with the oscillations of the electrical currents in the motor windings. In the first example the retarding torque described by (8) was assumed for $h=1$ and $z=1$, which denotes its two step-wise changes per one working tool revolution with an amplitude equal to the average retarding torque value. The time history plots of the driving and retarding torques normalized by the rated torque M_n during the start-up and the beginning of nominal operation are illustrated in Fig. 6a by the black and grey lines, respectively. The corresponding time histories of the motor rotor and the driven machine tool rotational speeds are presented in Fig. 6b also by the black and grey lines, respectively. From these plots it follows that the drive system of the

entire mass moment of inertia reduced on the motor shaft equal to 0.78 kgm^2 has been accelerated from its standstill to the nominal rotational speed in ca. 1 s. In Fig. 6c there is presented the system dynamic response in the form of time-history

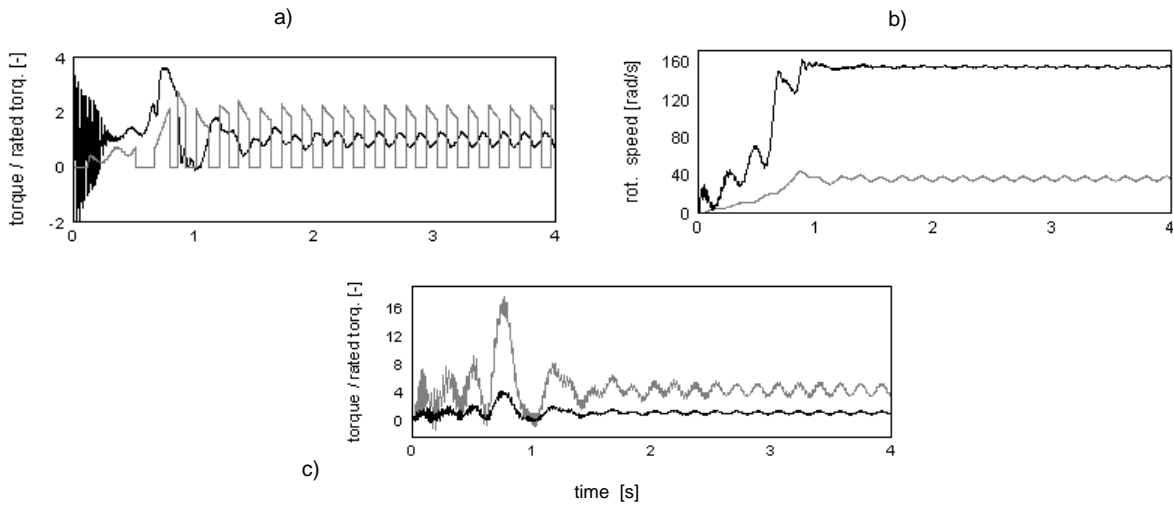


Figure 6: Time histories of the passive system dynamic response obtained for $k=1$ in (8).

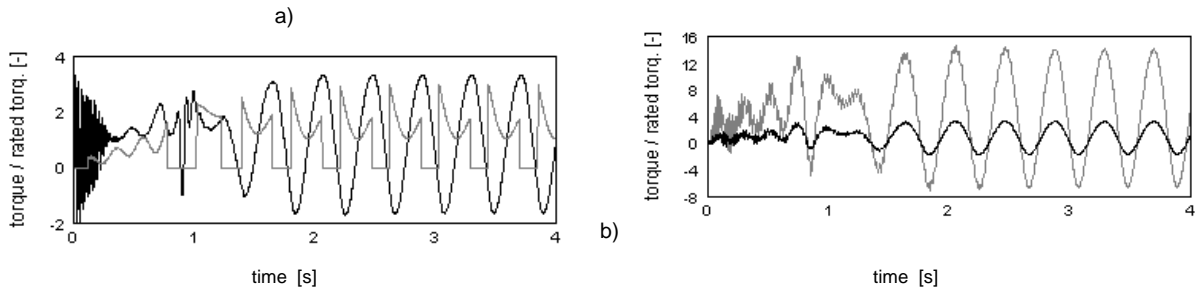


Figure 7: Time histories of the dynamic response obtained for the passive system for $k=0.425$ in (8).

plots of the dynamic torques transmitted by the drive system shaft segments in which the torque-meters are installed, where by the black line the result registered between the driving motor and the reduction planetary gear is plotted and by the grey line there is plotted the analogous result registered between the gear stage and the driven machine tool, see Fig. 2. From Fig. 6 it follows that upon the passage through the very severe transient excitation generated by the asynchronous motor the system starts to regularly oscillate according to the low-frequency fluctuation of the retarding torque with amplitudes remaining close to the quasi-static level. It is worth noting that the considered drive system is almost not sensitive to the typical transient excitation by the asynchronous motor of the network frequency 50 Hz, which can be explained by the positive influence of the three elastic couplings in the system resulting in the abovementioned hardly excited the third eigenfunction of the natural frequency 51.42 Hz shown in Fig. 4.

From all eigenfunctions presented in Fig. 4 for the system with the rigidly suspended gear housing as well as from numerous numerical simulations it follows that the considered drive system is particularly sensitive to low-frequency oscillations induced by fluctuation of the retarding torque generated by the pulverizer working tool, where the maximum dynamic response has been obtained for regular loading characterized by the fluctuation parameter $k=0.425$ in (8), which results in the excitation frequency equal to one half of the first system natural frequency $f_1 = 4.883$ [Hz]. This remarkable fact can be explained by the mentioned above non-linear electro-mechanical coupling effect resulting in such a sub-harmonic resonance. The simulation results obtained for this case are presented in the same way as above in Fig. 7 for the time-histories of the torques generated by the electric motor and the driven machine tool, Fig. 7a, as well as for the dynamic torques transmitted by the same shafts segments at the both torque-meter locations, Fig. 7b. Here, due to the systematically repeated jumps of the retarding torque the maximum amplitudes of the dynamic torques transmitted by the investigated input and output shafts are respectively almost 4 and 15 times greater than the rated torque, which is very dangerous for their fatigue durability and trouble-less operation. Moreover, apart from the strong dynamic torque fluctuation in the shafts, the induced by the considered electro-mechanical coupling very severe oscillation of the electromagnetic motor torque during the steady-state operation is also worth noting, Fig. 7a.

4. Control concepts of the transient and steady-state torsional vibrations

The first attempt to minimize the amplitudes of the transient and steady-state torsional vibrations occurring during start-ups and nominal operation of the coal pulverizer has been performed by using optimal constant values of the MRF actuator damping coefficients for the system with the visco-elastic support of the planetary gear housing. Since the investigated electro-mechanical object becomes non-linear in character, the applied e.g. in [3,4] methods of searching for the optimal constant damping coefficient values based on the frequency response functions can not be used here for this purpose. Thus, a search for the optimal constant damping coefficient values corresponding to the constant control voltages applied to the MRF actuators must have been reduced to numerous computational experiments in the form of numerical simulations carried out for the resonant operation conditions, i.e. for $k=0.425$ in (8), and for non-resonant working conditions, i.e. for $k=1$, of the considered drive system. Here, the fundamental criterion for the optimal constant C_0 in (2c), (4) and (5) are the minimal ‘peak-to-peak’ time-histories of the dynamic torques transmitted by the investigated input and output shafts. In Figs. 8a and 8b there are presented the time history plots of the dynamic torques transmitted by the mentioned shafts for the obtained in this way constant optimal damping coefficient $C_0=1125$ Ns/m per one MRF actuator, respectively for $k=0.425$ and for $k=1$. From the presented in these figures plots it follows that an elastic support of the planetary gear housing together with the constant damping coefficients of the MRF actuators result in $\sim 41\%$ smaller steady-state vibration amplitudes in the case of resonant operation and in remarkable, i.e. ca. 47%, attenuation of the transient vibrations during start-up in non-resonant conditions, where the following after it dynamic torque amplitudes in nominal working conditions remained on approximately the same quasi-static level, see Figs. 6c and 7c. In order to achieve a stronger suppression of torsional vibration amplitudes the semi-active control based on the closed-loop principle is required for this drive system.

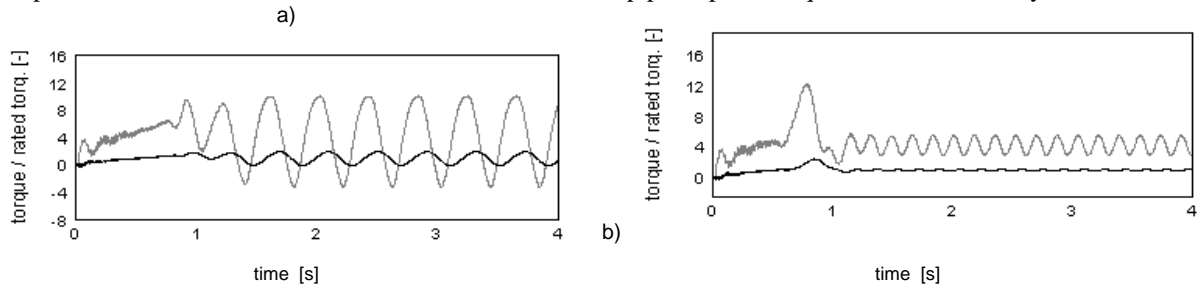


Figure 8: Time histories of the dynamic torques obtained for the optimal constant damping coefficient for the resonant (a) and non-resonant operation (b) of the drive system.

The dynamic responses obtained for the considered drive system are characterized by a severe domination of the first eigenform with a very weakly remarkable influence of the third eigenform and by a completely negligible influence of the remaining ones. Thus, in order to effectively suppress vibration amplitudes it is necessary to apply the analogous model-based approach as in [6] leading to elimination or at least minimization of the first mode external excitation $Q_1(t)$, which can be expressed by means of the following formula

$$Q_1(t) - \varepsilon \cdot a_{C1} C_0(t) \varphi_R(t) \rightarrow 0, \text{ where } Q_1(t) = a_{E1} T_{el}(t) - a_{R1} M_r(\Omega_r(t)), \varphi_R(t) = \sum_j \Phi_{Rj} \dot{\xi}_j(t) \quad (9)$$

and a_{C1} , a_{E1} , a_{R1} are the proper modal weighting coefficients for the system first eigenform, the MRF actuator resultant damping coefficient $C_0(t)$ consists of a constant value and a variable, response-dependent component, the forcing functions $T_{el}(t)$ and $M_r(\Omega_r(t))$ have been respectively defined by (7) and (8) and ε is the correction coefficient moderating the control function magnitudes for all eigenmodes taken into consideration. In practice, the theoretical expression (9) describing the first mode external excitation $Q_1(t)$ can be approximated with a reasonable accuracy by the being easily measured ‘on-line’ reaction torque occurring in the planetary gear housing visco-elastic support. Then, the variable damping coefficient $C_0(t)$ can be determined and upon proper ‘smoothing-out’ of the extremely high and small extreme peaks it can be substituted into equations (4) or (5) in order to simulate the system dynamic response. Here, the effectiveness of the semi-active control essentially depends on the correction coefficient ε related to the gear housing modal displacements Φ_{Rj} and r_{RS} ratio in (2a). The simulation results obtained for the most effective control and assuming realistic performances of the applied MR actuators [7] are presented in Figs. 9 and 10. In Fig. 9 there are demonstrated the analogous as before time-histories of the dynamic torques transmitted by the input and output shafts for the system in the resonant (Fig. 9a) and non-resonant (Fig. 9b) operation conditions. Fig. 10 illustrates the comparison between the rotational speed time-histories of the motor rotor and the driven machine tool obtained for the passive (Fig. 10a) and controlled (Fig. 10b) system. From the above plots it follows that by means of the semi-active control it was possible to significantly attenuate the torsional vibration amplitudes for the resonant operation both during the start-up and steady state process, where the dynamic torque fluctuations have been minimized to almost 25% of the respective passive system magnitudes, as shown in Fig. 7b. However, in the case of non-resonant operation the effects of the semi-active control are quite spectacular for the steady-state vibrations only, while the transient

components observed in Fig. 9b during the start-up became even more severe in comparison with the respective dynamic torque time-histories presented in Figs. 6c and 8b for the passive system and the optimal constant damping coefficient.

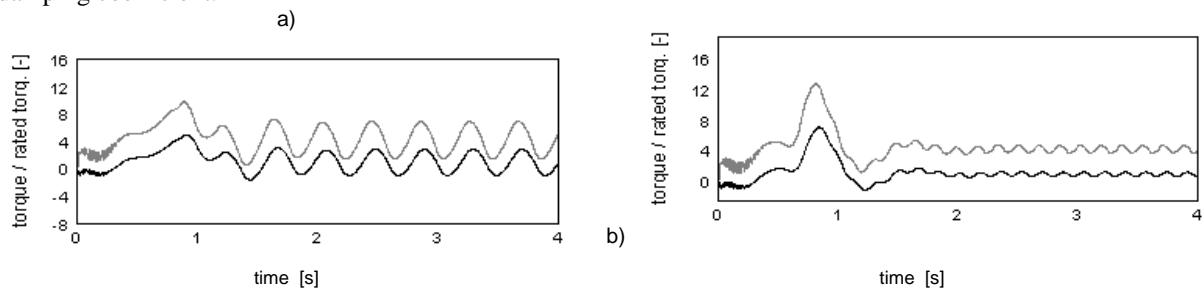


Figure 9: Time histories of the dynamic torques obtained using the semi-active control for the resonant (a) and non-resonant operation (b) of the drive system.

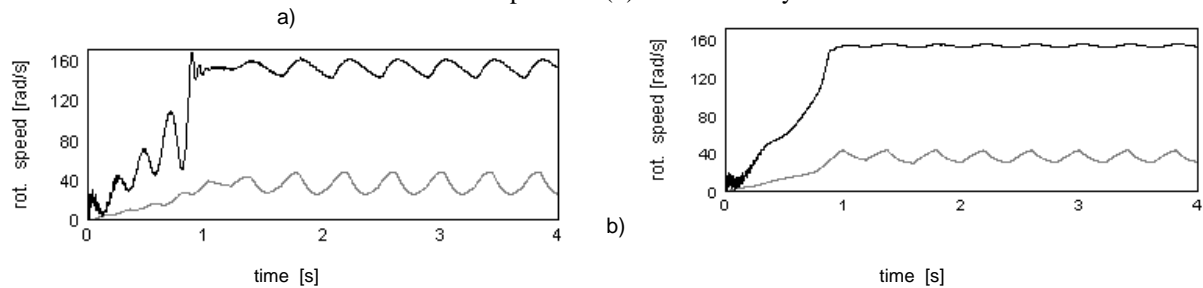


Figure 10: Time histories of the rotational speeds of the motor rotor and the driven machine tool obtained for the passive (a) and for the semi-actively controlled (b) drive system in resonant operation conditions.

Conclusions

In the paper a control of transient and steady-state torsional vibrations of the coal pulverizer drive system driven by the asynchronous motor and the planetary reduction gear has been performed by means of the linear dampers with the magneto-rheological fluid (MRF). Here, the control dampers are able to suppress the torsional vibrations by an introduction of mechanical energy dissipation during relative rotational motion between the planetary gear housing and the immovable foundation. As it follows from the numerical simulations carried out by means of two various electro-mechanical models, such actuators can effectively reduce the transient and steady-state torsional vibrations of the drive system not only using semi-active control in the form of closed-loop principle but also for the selected optimal constant damping coefficient of the magneto-rheological fluid.

In the next step of research in this field the results of theoretical investigations are going to be experimentally verified by the use of the being currently under construction real coal pulverizer drive system described above. Moreover, the semi-active control will be focused on stochastic external loadings imposed to the driven machine.

Acknowledgement

These investigations are supported by the Polish National Centre of Research and Development of the Ministry of Science and Higher Education: Research Project PBR- N R03 0012 04.

References

- [1] Laschet, A. (1988): *Simulation von Antriebssystemen*. Springer-Verlag, Berlin, London, New-York, Paris.
- [2] Przybyłowicz, P. M. (1995): Torsional vibration control by active piezoelectric system. *J. of Theoretical and Applied Mechanics*, 33(4), pp. 809-823.
- [3] Szolc, T. and Jankowski, Ł. (2009): Semi-active control of torsional vibrations of drive systems by means of actuators with the magneto-rheological fluid. *Proc. of 8th International Conference on Vibrations in Rotating Machines - SIRM 2009*, Vienna, Austria, 23 - 25 February 2009, Paper ID-25.
- [4] Szolc, T., Jankowski, Ł., Pochanke, A., Magdziak, A. (2010): An application of the magneto-rheological actuators to torsional vibration control of the rotating electro-mechanical systems. *Proc. of the 8th IFToMM Int. Conference on Rotordynamics*, September 12-15, 2010, KIST, Seoul, Korea (*in print*).
- [5] White, D. C. and Woodson, H. H. (1959): *Electromechanical energy conversion*. New York: Wiley.
- [6] Frischgesell, T., Popp, K., Szolc, T., Bogacz, R. (1994): Active control of elastic beam structures. *Proc. of the IUTAM Symposium: The Active Control of Vibrations*, Bath, Great Britain, Sept.1994, pp. 115-122.
- [7] Mikułowski, G., Holnicki-Szulc, J. (2007): Adaptive landing gear concept – feedback control validation. *Smart Materials and Structures*, 16(6), pp. 2146-2158.